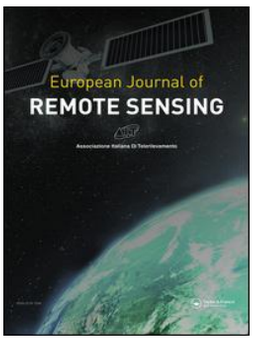

European Journal of Remote Sensing

ISSN: (Print) 2279-7254 (Online) Journal homepage: http://www.tandfonline.com/loi/tejr20

Assessing in-season crop classification performance using satellite data: a test case in Northern Italy

Ramin Azar, Paolo Villa, Daniela Stroppiana, Alberto Crema, Mirco Boschetti & Pietro Alessandro Brivio

To cite this article: Ramin Azar, Paolo Villa, Daniela Stroppiana, Alberto Crema, Mirco Boschetti & Pietro Alessandro Brivio (2016) Assessing in-season crop classification performance using satellite data: a test case in Northern Italy, European Journal of Remote Sensing, 49:1, 361-380, DOI: 10.5721/EuJRS20164920

To link to this article: http://dx.doi.org/10.5721/EuJRS20164920

Published online: 17 Feb 2017.

European Journal of Remote Sensing - 2016, 49: 361-380
doi: 10.5721/EuJRS20164920
Received 07/03/2016 accepted 21/06/2016

European Journal of Remote Sensing
An official journal of the Italian Society of Remote Sensing

www.aitjournal.com

Assessing in-season crop classification performance using satellite data: a test case in Northern Italy

Ramin Azar, Paolo Villa*, Daniela Stroppiana, Alberto Crema, Mirco Boschetti and Pietro Alessandro Brivio

Institute for Electromagnetic Sensing of the Environment (IREA), National Research Council (CNR), Via E. Bassini, 15, I-20133, Milan, Italy
*Corresponding author, e-mail address: villa.p@irea.cnr.it

Abstract
This study investigated the feasibility of delivering a crop type map early during the growing season. Landsat 8 OLI multi-temporal data acquired in 2013 season were used to classify seven crop types in Northern Italy. The accuracy achieved with four supervised algorithms, fed with multi-temporal spectral indices (EVI, NDFI, RGRI), was assessed as a function of the crop map delivery time during the season. Overall accuracy (Kappa) exceeds 85% (0.83) starting from mid-July, five months before the end of the season, when maximum accuracy is reached (OA=92%, Kappa=0.91). Among crop types, rice is the most accurately classified, followed by forages, maize and arboriculture, while soybean or double crops can be confused with other classes.
Keywords: Early mapping, crop type, multi-temporal data, supervised classification, Landsat 8 OLI.

Introduction
Observation and assessment of crop status and development is a crucial topic for agronomic planning and management and for mitigating the effects induced by climate change and extreme events. To this aim, timely information on the area covered by different crops is necessary [Foerster et al., 2012; Conrad et al., 2014]. In particular, in-season crop type maps produced during early growth stages are key information for operational agricultural monitoring by both public authorities and private sector. In southern Europe, where irrigated agriculture is the major user of fresh water resources [Rost et al., 2008; Wriedt et al., 2009], early information on crop type and acreage is necessary to forecast agricultural water demand during the summer season [Mo et al., 2005; Reichstein et al., 2007]. Despite the need for information delivered in near-real time during the crop season, official figure and statistics are usually provided after the end of the growing season, since data have to be collected, verified and compiled into a database.
Satellite remote sensing is a unique source of data for the identification of crop types over large areas, as described in the last two decades in scientific literature [e.g. Ortiz et al.,

1997; Pohl and Van Genderen, 1998; De Wit and Clevers, 2004; Ok et al., 2012; Villa et al., 2015]. A number of factors influence the accuracy of satellite-based crop maps: i.e. the spatial resolution of the imagery, the classification method, and the production time horizon, i.e. the temporal extent of the dataset and phenological stages covered [Hubert-Moy et al., 2001; Van Niel and McVicar, 2004; Duveiller and Defourny, 2010]. Cultivated crops and site characteristics regulate the selection of the most suitable satellite dataset. Low/moderate resolution sensors with frequent revisit (300-1000 m, e.g. MODIS) are best suited for assessing inter-annual variability over large, homogeneous areas [e.g. Wardlow and Egbert, 2008], while medium resolution data (10-30 m, e.g. Landsat) give better results at local/regional scales and over fragmented landscapes [e.g. Murty et al., 2003; Conrad et al., 2014]. Duveiller and Defourny [2010] and Yang et al. [2011] demonstrated that spatial resolution in the range 10-140 m could be considered an optimal choice for a wide range of agricultural landscapes.

Vegetation indices (VIs) have been largely used for monitoring vegetation over a wide range of applications [e.g. Huete et al., 1994; Gitelson and Merzlyak, 1996; Nutini et al., 2013; Villa et al., 2014]. They offer a straightforward way of feature reduction in high dimensional datasets and are easily interpretable proxies of vegetation processes and agro-practices. Multi-temporal studies focusing on in-season crop type mapping revealed that maximum discrimination capabilities occurs at different phenological stages and that great attention must be devoted to missing data at key dates along the growing season [Odenweller and Johnson, 1984; Murthy et al., 2003; Conrad et al., 2014].

In order to fill the gap towards operational use of satellite products for crop monitoring, more research is needed for evaluating timely crop mapping, and in particular experimental studies fully taking into account local agricultural practices and variability. New generation medium resolution satellite platforms recently put into orbit, e.g. Landsat 8 [Irons et al., 2012] and Sentinel-2 [Drusch et al., 2012], will provide a large amount of data featuring spatial and temporal resolutions with great potential for advancing science and technology towards effective in-season crop mapping.

In this framework, the objective of this work is to investigate the performance of crop type classification as a function of the time of crop map delivery during the season (i.e. early season and end of season maps) over Lombardy, one of the most important extensive agricultural region in Italy. To this aim, we tested four common supervised classification algorithms (Maximum Likelihood, Minimum Distance, Spectral Angle Mapper and Neural Networks) [Kruse, 1993; Richards, 1999], applied to multi-temporal VIs derived from medium resolution satellite data (i.e. Landsat 5, 7 and 8). The main outcome focuses on how early in the growing season a reliable crop type map could be produced, as an operational remote sensing product targeted at regional agricultural monitoring.

Study site

The study area is located in the central portion of Lombardy region, Northern Italy, and covers more than 10,000 km². The area, highlighted by the light blue box in Figure 1, was selected in the overlapping region of two Landsat WRS-2 paths (193 and 194), in order to guarantee frequent observations of the surface by the Landsat overpass (up to 7-9 day frequency). Such dataset is considered a good compromise between spatial resolution [Duveiller and Defourny, 2010] and temporal revisit for simulating an operational crop

mapping scenario, possibly exploiting the future availability (2017-2018) of optical satellite such as Sentinel-2 and Landsat 8 missions.

Lombardy region is among the most urbanized areas in Europe, hosting around 10 million people, yet 41.4% of its territory is dedicated to agriculture. The added value of agro-industrial sector for regional economy is 15% of the national total. The region is mostly flat, except for the northernmost regions located in the Alps, and agriculture is the dominant land use especially in the southern Po plain. Climate is continental, with some variability due to altitude in northern mountainous areas and near the large pre-Alpine lakes, with accentuated annual temperature changes in the plains and precipitations that are ranging from 600 to 1000 mm/year (850 mm/year on average).

Vegetated land cover is quite heterogeneous, including woodland and arboriculture, grassland, horticulture, viticulture, winter and summer crops, forage crops and permanent meadows. According the National Institute of Agricultural Economics [Giuca et al., 2014] the main crops cultivated in Lombardy are: maize (38.5% of total cropland area), temporary and permanent meadows for forages (34.1%), rice (10.1%), winter cereals (common wheat and barley, 7.5%), soybean and other legumes (2.7%), vegetables (1.4%).

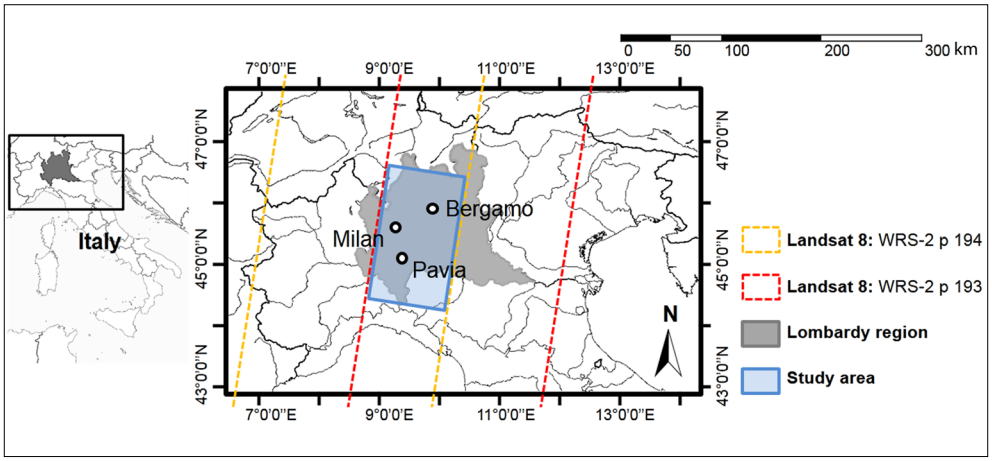

Figure 1 - Study area coverage (light blue box), bounded by overlapping of WRS-2 194 and 193 paths of Landsat 8 orbits.

Two major crop seasons can be identified in the area: October to June for winter crops and April to October for summer crops. A graphical crop calendar is shown in Figure 2. Winter cereals, being barley the most cultivated one, are sown between October and November, typically reach the flowering in April-May of the following year, and are harvested in May-June. Maize and rice are the main summer crops that cover the majority (~ 50%) of cultivated area and they are more demanding in term of water consumption. Maize is sown between early April and the beginning of May: the crop reaches the peak of vegetative phase around July and it is harvested between late August and the second half of September. Rice is usually sown later than maize, from middle of April to late May, reaching flowering stage in late July-August, and is harvested in late September-beginning of October. Double

cropping practices concern maize and soybean that are sown as second crop in late May or early June, after the harvest of forage crops (e.g. ryegrass) or winter cereals (e.g. triticale); double crops are typical of integrated crop-livestock systems (e.g. for Parmesan cheese production) in which they are used either as fresh forage or silage. Other forage crops cultivated in the area mainly consist of grasses (i.e. ryegrasses) and herbaceous legumes (i.e. alfalfa and clovers), which are mowed and harvested three to four times, with nearly monthly frequency, during May to August period. Arboriculture is mainly consisting of poplar plantations for pulpwood, used in construction, paper production and biomass for power plants.

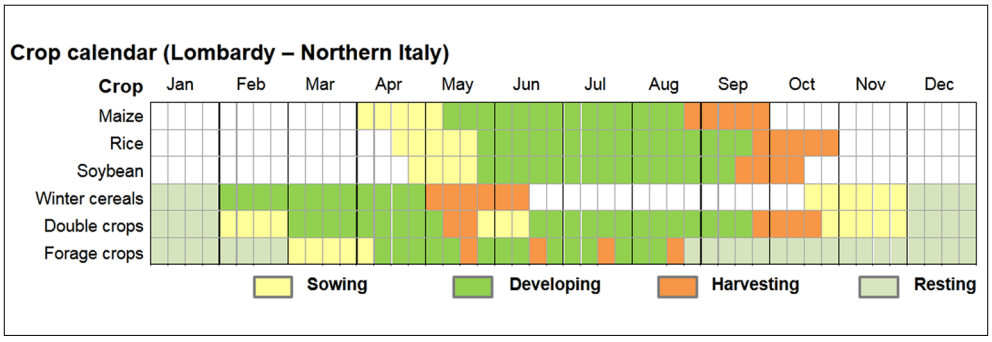

Figure 2 - Typical crop calendar for major cultivations in Lombardy (Northern Italy).

Dataset

Satellite data

26 Landsat 8 Operational Land Imager (OLI) individual scenes were collected for the year 2013, covering the WRS-2 194-193/28-29 path/row (Fig. 1). The overlap between the two adjacent WRS-2 paths assures an enhanced temporal frequency of satellite coverage from 16 days to 7-9 days, if cloud free images are available. Landsat 8 OLI scenes were retained only when overall cloud cover was less than 20%. Panchromatic and thermal infrared OLI bands were discarded and reflective bands at 30 meters spatial resolution were processed. The study period covers the summer crop season, which is the most important one for agriculture in Lombardy; in this period in fact the main crops are cultivated (rice and maize) and water demand and water resource management are major issues for decision makers. Hence, the temporal range of interest is spanning from sowing (April) to harvest (October) of major summer crops in Northern Italy. Landsat 8 OLI is operational since April 2013, but the first cloud free image over our study area was collected on May, 13th. The multi-temporal dataset collected for the year 2013 spans 13 dates (two OLI scenes for each date) with a temporal interval between consecutive cloud free acquisitions in the range of 7-16 days, with the exception of the first two dates of the series which are 25 days apart (Tab. 1).

Table 1 - The Landsat 8 OLI dataset acquired over the study area for the year 2013. Time step datasets (T) effectively considered for the classification are reported as progressive number (T1 to T8) according the cardinality of dates included.

Path	Row	Date (DOY)	T1	T2	T3	T4	T5	T6	T7	T8
194	28-29	13/05/2013 (133)	x	x	x	x	x	x	x	x
193	28-29	07/06/2013 (158)	x	x	x	x	x	x	x	x
194	28-29	14/06/2013 (165)	x	x	x	x	x	x	x	x
193	28-29	23/06/2013 (174)	x	x	x	x	x	x	x	x
194	28-29	30/06/2013 (181)	x	x	x	x	x	x	x	x
194	28-29	16/07/2013 (197)		x	x	x	x	x	x	x
193	28-29	25/07/2013 (206)			x	x	x	x	x	x
194	28-29	01/08/2013 (213)				x	x	x	x	x
193	28-29	10/08/2013 (222)					x	x	x	x
194	28-29	17/08/2013 (229)						x	x	x
194	28-29	02/09/2013 (245)							x	x
194	28-29	07/12/2013 (341)								x
193	28-29	16/12/2013 (350)								x
			T1	**T2**	**T3**	**T4**	**T5**	**T6**	**T7**	**T8**

Reference data

For calibration and validation purposes, we used independent crop type reference data derived on the basis of the "Annual agricultural land use map" (Carta Uso Agricolo Annuale, CUAA) produced by the "Ente Regionale per i Servizi all'Agricoltura e alle Foreste" (i.e. the regional agency for agriculture and forest services of the regional government) over Lombardy. This map elaborates information from 2013 farmers' declarations for requesting European subsidy (http://www.ersaf.lombardia.it/servizi/Menu/dinamica.aspx?idArea=16914&idCat=17255&ID=22103) and is usually published at the beginning of the year following the summer crop season, i.e. about four to five months after the harvest. The crop categories mapped in CUAA 2013 represent crop information not semantically consistent with crop classes that can be detected on the basis of optical spectral response from remote data. For example, the CUAA crop category maize includes both maize cultivated as single and double crop, while the category forages includes every crop which is cultivated for animal consumption, including some winter cereals, as well as fodder and meadows (alfalfa and similar), which is grown and mowed multiple times per season. Moreover, CUAA product is not officially validated. For the above reasons, this data is considered not enough reliable to be used as reference data directly by itself, without prior check. Therefore, CUAA 2013 map was used as base information for extracting a sample of fields, which have been further checked for crop type label attribution. A random sample of fields stratified by 6 vegetated land cover classes (5 crop types: maize, rice, soybean, winter crops, and forages, plus natural and artificial woodland areas) was extracted from

CUAA 2013. Class label attribution consistency check was carried out using additional information: i.e. visual assessment of high resolution satellite photos (from Google Earth), and *in situ* collected information (along the road survey with camera and GPS, especially for rice fields identification and flooding status assessment). Finally, *in situ* collected information and expert interpretation of VIs multi-temporal profiles extracted from OLI scenes were used for separating the double from single crops and for further subdividing of crop type classes according to their seasonality (e.g. early seeded *vs*. late seeded maize), thus delineating a detailed reference set composed by 15 crop type classes.

Methods

OLI data were converted to at-sensor radiance using calibration coefficients provided within the scenes metadata and transformed to surface reflectance with the Atmospheric/Topographic CORrection (ATCOR) software [Richter and Schläpfer, 2011]. For atmospheric correction, we adopted Aerosol Optical Depth (AOD) parameters derived as a weighted average of two AERONET stations measurements: Ispra, (45.803° N, 8.627° E, elevation: 235 m) and Modena (44.632° N, 10.945° E, elevation: 56 m); the MODIS aerosol products (MOD04_L2) were used when AERONET data were missing. After atmospheric correction, only the area overlapping WRS-2 paths 193 and 194 was used as input for the processing workflow (Fig. 3).

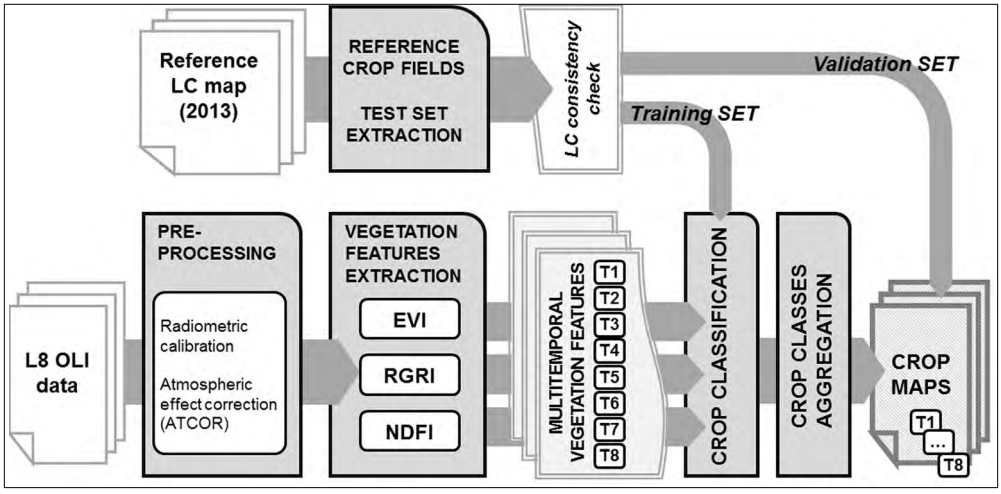

Figure 3 - The flowchart of the crop mapping methodological approach.

Three spectral VIs were calculated from each date of OLI 2013 dataset: Enhanced Vegetation Index (EVI) [Huete et al., 1997], Normalized Difference Flood Index (NDFI) [Boschetti et al., 2014], and Red Green Ratio Index (RGRI) [Gamon and Surfus, 1999]. Multi-temporal VIs, in particular Normalized Difference Vegetation Index (NDVI), have been extensively used in remote sensing of vegetation for their availability, simplicity and effectiveness in distinguishing phenological features of plant groups, including crops [e.g. Lunetta et al., 2006; Waldrow and Egbert, 2008]. As NDVI can be subject to distortion due to environmental factors, for our analysis we preferred to use EVI, which includes a factor for correcting background effects and partially compensating for major atmospheric

disturbances [Huete et al., 1997]. As a complement to EVI, we included NDFI, which is an index developed by Boschetti et al. [2014] for the detection of surface water in flooded rice areas, modified for optimizing the performance of indices previously used by Xiao et al. [2005] for mapping paddy rice cultivations. The RGRI was included due to its sensitivity to canopy greenness and light use efficiency in plant photosynthetic activity [Gamon and Surfus, 1999]. Differently from other indices of this category, relying on hyperspectral information, RGRI can be computed from the spectral bands available from OLI [e.g. Gamon et al., 1992; Gitelson and Marzlyak, 1996]. The equations used for calculating the three VIs using reflectance (ρ) derived from OLI spectral bands are:

$$EVI = 2\frac{\rho_{NIR(OLI\ band\ 5)} - \rho_{Red(OLI\ band\ 4)}}{\rho_{NIR(OLI\ band\ 5)} + 6\rho_{Red(OLI\ band\ 4)} - 7.5\rho_{Blue(OLI\ band\ 2)} + 1} \quad [1]$$

$$NDFI = \frac{\rho_{Red(OLI\ band\ 4)} - \rho_{SWIR2(OLI\ band\ 7)}}{\rho_{Red(OLI\ band\ 4)} + \rho_{SWIR2(OLI\ band\ 7)}} \quad [2]$$

$$RGRI = \frac{\rho_{Green(OLI\ band\ 3)}}{\rho_{Red(OLI\ band\ 4)}} \quad [3]$$

From the whole dates of acquisition of OLI data, eight 'time step' datasets (T1-T8) were composed by stacking layers of the three VIs from the first up to the last date of each step (Tab. 1). The first time step, T1, includes the earliest 5 dates, from May 13th to June 30th, 2013; at each following step one date is added to the multi-temporal dataset up to T7. At step T8 (13 dates) the entire crop growing season is covered, including harvest (218 days, from May 13th to December 16th). Among the time steps, T2 (up to July 16th) and T3 (up to July 25th) are assumed as potential horizons for delivering early in-season crop maps that could be used in support of crop management, i.e. before water demand peak of major summer crops in the study area (rice and maize) and last top-dressing fertilization.

Four supervised classification algorithms, three parametric and one non-parametric, were used: Maximum Likelihood Classification (MLC) [Richards, 1999], Euclidean Minimum Distance (EMD) [Richards, 1999], Spectral Angle Mapper (SAM) [Kruse et al., 1993] and Neural Networks (NN) [Richards, 1999]. All of these algorithms are coded in IDL and embedded in ENVI 4.7 software package. These algorithms well represent a variety of supervised approaches usually employed for classification purposes in remote sensing literature: MLC is a parametric algorithm, based on the conditional distribution of classes, EMD is a geometry-based algorithm using a distance metric, SAM is based on angular distance in n-dimensional space, and NN is non-parametric and non-linear algorithm based on feed-forward back-propagation learning.

Training and validation sets were selected as described in Dataset section by extracting a stratified random sample of field polygons from reference crop type data, belonging to 15

crop classes, to cover the variability of crop types within the study area (Tab. 2). Two-thirds of the fields were used for training, and the remaining third for validation of crop mapping results. Classification algorithms were applied to each time step dataset for mapping the 15 crop classes, which were later aggregated to 7 classes to produce the final crop maps (Tab. 2). Arboriculture-woodland is a unique class, merging tree farming areas and natural woodland. Since our focus is on the assessment of crop type classification performance, crop type maps are produced only over vegetated areas. For this reason, CUAA 2013 map was used to mask out non-cropland (non-vegetated) areas, such as urban areas and water bodies, and the classification tests were run only over vegetated areas (i.e. covered by agricultural crops or natural vegetation).

Table 2 - Training and validation set description, highlighting crop type and land cover class targets.

Crop type/category description		Training fields (px)	Validation fields (px)	Aggregated class
1	Early maize	142 (2073)	71 (1733)	Maize
2	Medium maize			
3	Late maize			
4	Early rice	113 (2528)	58 (1328)	Rice
5	Late rice			
6	Dry seeded rice			
12	Early soybean	52 (1144)	21 (486)	Soybean
13	Late soybean			
7	Winter cereals	112 (2825)	31 (773)	Winter crop
8	Double crop (winter crop + maize)		40 (1039)	Double crop
9	Double crop (winter crop + other)			
10	Fodder	72 (1713)	40 (1039)	Forages
11	Grassland pasture			
14	Tree farming and woodland (short trees)	70 (2082)	26 (671)	Arboriculture-woodland
15	Tree farming and woodland (tall trees)			

The four classifiers were applied separately to all the time step datasets (T1 to T8) and the output crop maps have been validated by comparison with the validation set, using the confusion matrix approach [Congalton, 1991]. The following accuracy metrics were computed: Overall Accuracy (OA), Kappa coefficient of agreement (***k***), per-class User's (UA) and Producer's (PA) Accuracy, as well as Commission (CE) and Omission (OE) errors.

Results

Crop mapping accuracy and delivery time

Table 3 reports OA and ***k*** values together with the percentage change between two consecutive time steps as provided by the four classification algorithms. MLC is the best performing algorithm with OA>78% and ***k***>0.73, already since the first time step T1 (end of June, 5 dates) followed by NN with OA > 71% and ***k*** > 0.66. A t-test revealed that MLC and NN OA scores are significantly different ($\alpha = 0.05$) for all time step except T2 (t=0.067)

and T8 (t=0.106). SAM and EMD achieved lower accuracy with OA (at T2 to T3) 12-14% lower than MLC and NN classifications.

Table 3 - Overall accuracy (OA) and Kappa coefficient (*k*) for the four classification methods, expressed as values for each time step (Tn) and change with respect to the previous time step (Tn-1).

		MLC		NN		EMD		SAM	
		Value	**Change**	**Value**	**Change**	**Value**	**Change**	**Value**	**Change**
T1 (30/06)	OA	78.0%	-	71.8%	-	62.4%	-	63.7%	-
	k	*0.737*	-	*0.660*	-	*0.547*	-	*0.563*	-
T2 (16/07)	OA	86.5%	+8.5%	85.5%	+7.9%	70.3%	+11.6%	75.3%	+13.7%
	k	*0.838*	*+0.101*	*0.825*	*+0.095*	*0.641*	*+0.140*	*0.703*	*+0.165*
T3 (25/07)	OA	88.5%	+2.0%	87.1%	+4.5%	74.8%	+1.5%	76.8%	+1.6%
	k	*0.862*	*+0.024*	*0.845*	*+0.056*	*0.697*	*+0.018*	*0.721*	*+0.019*
T4 (01/08)	OA	89.4%	+0.9%	88.1%	+1.2%	76.0%	+1.1%	77.8%	+1.0%
	k	*0.872*	*+0.010*	*0.857*	*+0.015*	*0.712*	*+0.012*	*0.733*	*+0.012*
T5 (10/08)	OA	91.1%	+1.7%	88.3%	+1.2%	77.2%	+0.8%	78.7%	+0.2%
	k	*0.893*	*+0.021*	*0.859*	*+0.013*	*0.726*	*+0.009*	*0.742*	*+0.002*
T6 (17/08)	OA	90.9%	-0.2%	89.1%	+1.2%	78.4%	+0.7%	79.3%	+0.8%
	k	*0.891*	*-0.002*	*0.868*	*+0.014*	*0.740*	*+0.008*	*0.750*	*+0.010*
T7 (02/09)	OA	92.6%	+1.7%	90.7%	+0.3%	78.7%	+0.5%	79.8%	+1.6%
	k	*0.912*	*+0.021*	*0.888*	*+0.003*	*0.743*	*0.006*	*0.756*	*+0.019*
T8 (16/12)	OA	92.7%	+0.1%	92.7%	+3.3%	82.0%	+1.8%	81.6%	+2.0%
	k	*0.912*	*+0.001*	*0.912*	*+0.040*	*0.783*	*+0.022*	*0.778*	*+0.024*

OA and ***k*** generally increase from T1 to T8 for all classification algorithms; the only minor exception is MLC at T6 which has a 0.2% OA decrease (-0.002 for ***k***) with respect to T5. For all the classification methods, the lowest OA (***k***) scores are observed at T1 (only five images in the dataset, with 15 input features) with minimum of 62.4% (0.55) and maximum of 78.0% (0.74) for EMD and MLC classifiers, respectively. Conversely, OA (***k***) scores reach the highest values when the multi-temporal dataset is complete (T8, 13 dates, 39 input features). In particular, on the upper bound MLC and NN classifications converge to the same accuracy (OA=92.7%, ***k***=0.91), while on the lower bound SAM and EMD classifications converge to similar scores (OA ~ 82.0% and ***k*** ~ 0.78).

The largest accuracy increment is observed between T1 (end of June) and T2 (mid of July), for all classifiers with OA increments ranging from 7.9% to 13.7%. Best performing MLC classifications reach OA = 86.5% (***k***=0.84) at T2, compared to OA = 78.0% (***k***=0.74) scored at T1, and a further OA gain of +2% is observed adding the end of July OLI scene (T3). The additional information brought by post-harvesting scenes (T8) finally increases OA and ***k*** by a significant amount with respect to T7 (beginning of September), with the exception of MCL (+0.1% in OA).

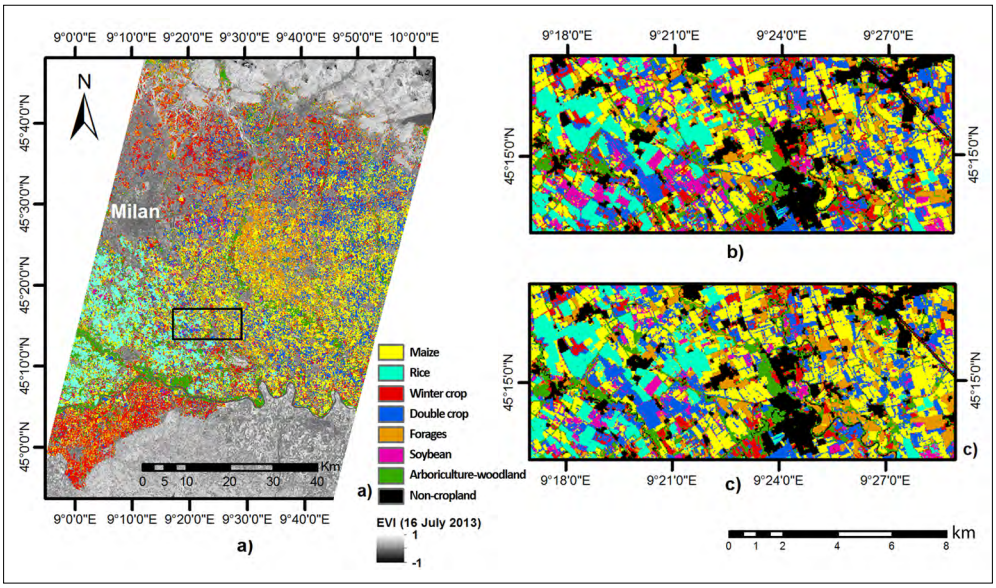

Figure 4 - The crop map derived with the MCL algorithm at T8 overlaid on EVI layer for July 16th, 2013 (a), and a zoom over the study area showing a detail of the crop maps derived with the MLC algorithm at T2 (b) and T8 (c). The rectangle area in panel a shows the extent of the zoom area.

Figure 4 shows the crop map derived with the MCL algorithm at T8 (panel a); in the two zoom rectangles, the MCL classification at T2 (i.e. early in-season map, panel b) and T8 (i.e. end of season map, panel c); urban areas and other non-arable land cover classes are displayed in black colour. The principal cropping systems in the area can be identified in Figure 4a: i) the rice district in the south-western part of the study area (cyan colour); ii) Maize and Forages are distributed in the central part (yellow and orange colour), with some Double crop and Winter crop patches (blue and red colour); and iii) winter crops are the major cultivation south of Po river (red colour, lower left in Fig. 4a). Areas classified as natural vegetation (included into Arboriculture-woodland class) can be observed as light green belts along the Po river, the Ticino river (flowing into the Po river from the west) and the Adda river (crossing the study area from North to South). In the detailed Figures 4b-c the patterns of the rice fields (cyan colour) mapped at T2 and T8 are consistent with each other while the Double crop class tends to increase in coverage at time T8 (Fig. 4c).

Per-class accuracy

Figure 5 shows per-class commission (CE) and omission (OE) errors for each considered time step and algorithm. Commission and omission errors in the MLC and NN classifications are generally lower than 25% after T3 (i.e. up to July 25th); the exceptions are Soybean and Double crop classes derived with NN algorithm, with OE > 25%. The Soybean class is the worst classified class, with CE and OE greater than 70% for EMD, NN and SAM at T1. Even with the best performing algorithm, i.e. MCL, CE is higher than 50% at T1 for the Soybean class, although it rapidly decreases below 25% after T2. As shown by the confusion matrices (Tab. 4), Soybean pixels are mainly confused with Maize (and vice-

versa) at the earlier stages (T1 to T3). OE for Soybean at T8 is still around 25% for all classification algorithms, due to residual confusion with Maize. CE for Soybean at T8 are lower in the case of MCL and NN algorithms.

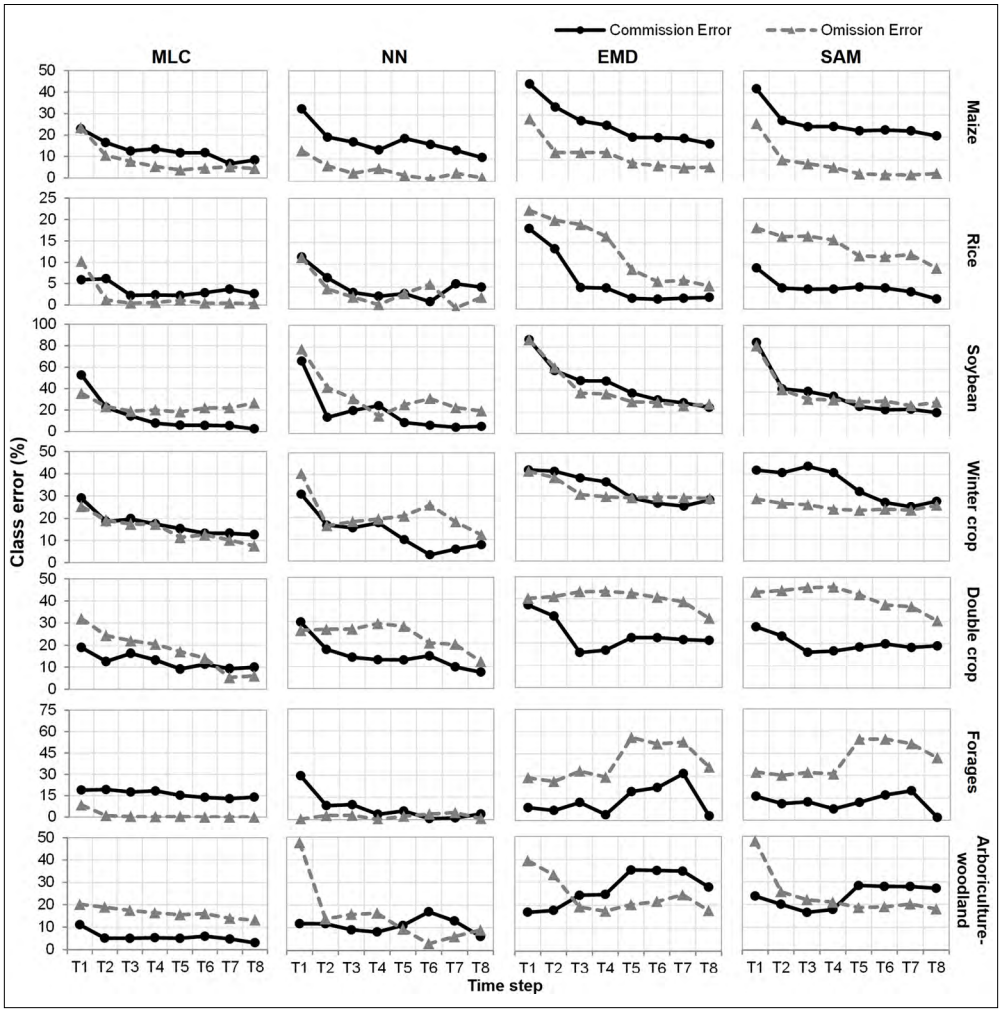

Figure 5 - The commission (CE, black line) and omission (OE, dotted grey line) errors (y-axis [%]) as a function of the time step (x-axis), derived with the four classification methods (columns) and for each target crop type (rows). For enhancing readability, the scale of y-axis varies with the crop type.

At T1 Double crop are mistakenly classified as Winter crop, and misclassifications of Soybean and Double crop classes strongly contribute to the lower overall accuracy observed (Tab. 3) when using multi-temporal data only up to June 30th.

Table 4 - Confusion matrices for crop maps produced using MLC and EMD algorithms, at T2 and T8 time steps. Class accuracies (Producer's and User's) lower than 80% are highlighted in grey.

		Reference dataset							
		Maize	**Rice**	**Soyb.**	**W. crop**	**D. Crop**	**Forages**	**Arbor.**	***User's Accuracy***
MCL (T2)	Maize	**1550**	8	111	30	145	0	12	***83.5%***
	Rice	57	**1312**	1	3	19	0	6	***93.9%***
	Soybean	78	8	**515**	2	52	0	9	***77.6%***
	Winter crop	6	0	18	**626**	37	3	78	***81.5%***
	Double Crop	25	0	24	37	**786**	0	27	***87.4%***
	Forages	0	0	0	51	0	**481**	64	***80.7%***
	Arboriculture-woodland	17	0	2	24	0	2	**839**	***94.9%***
	Producer's Accuracy	***89.4%***	***98.8%***	***76.8%***	***81.0%***	***75.7%***	***99.0%***	***81.1%***	OA=86.5% ***k***=0.838
MCL (T8)	Maize	**1657**	4	83	0	62	0	2	***91.7%***
	Rice	19	**1324**	14	3	0	0	0	***97.4%***
	Soybean	12	0	**493**	0	0	0	0	***97.6%***
	Winter crop	0	0	0	**714**	0	0	103	***87.4%***
	Double Crop	22	0	65	19	**976**	0	2	***90.0%***
	Forages	11	0	16	21	1	**486**	30	***86.0%***
	Arboriculture-woodland	12	0	0	16	0	0	**898**	***97.0%***
	Producer's Accuracy	***95.6%***	***99.7%***	***73.5%***	***92.4%***	***93.9%***	***100%***	***86.8%***	OA=92.7% ***k***=0.912
EMD (T2)	Maize	**1504**	145	317	17	177	2	106	***66.3%***
	Rice	116	**1062**	14	31	0	0	6	***86.4%***
	Soybean	106	77	**263**	31	98	0	53	***41.9%***
	Winter crop	0	0	20	**476**	149	103	64	***58.6%***
	Double Crop	2	44	57	99	**613**	0	89	***67.8%***
	Forages	0	0	0	0	0	**358**	26	***93.2%***
	Arboriculture-woodland	5	0	0	119	2	23	**691**	***82.3%***
	Producer's Accuracy	***86.8%***	***80.0%***	***39.2%***	***61.6%***	***59.0%***	***73.7%***	***66.8%***	OA=70.3% ***k***=0.641
EMD (T8)	Maize	**1617**	14	72	7	168	0	73	***82.9%***
	Rice	17	**1259**	9	0	0	0	8	***97.4%***
	Soybean	96	23	**489**	0	25	12	0	***75.8%***
	Winter crop	0	0	0	**550**	120	3	93	***71.8%***
	Double Crop	0	32	91	0	**715**	69	0	***78.8%***
	Forages	0	0	0	1	0	**311**	9	***96.9%***
	Arboriculture-woodland	0	215	0	91	11	10	**852**	***72.1%***
	Producer's Accuracy	***93.3%***	***94.8%***	***72.9%***	***71.2%***	***68.8%***	***64.0%***	***82.3%***	OA=82.0% ***k***=0.783

In the MLC classifications, Rice and Arboriculture-woodland are characterized by the lowest commission (<10%) and Rice and Forages by the lowest omission (<10%) errors. As a general trend, CE is higher than OE for Maize and Forages, and OE is higher than CE for Double crop, Arboriculture-woodland and Soybean. The lowest difference between CE and OE is observed for Rice and Winter crop for all time steps.
Commission and omission errors for EMD and SAM classifications are significantly greater than for MLC and NN, with the worst performance scored by EMD. The lowest CE and OE is generally achieved at T8, except for Forages which in EMD and SAM scores errors greater than 30% with increasing trend from T4. SAM performs better than MLC only for Forages up to T5 in terms of CE, and generally shows the highest CE and OE for all other classes, similarly to EMD.

Performance over major crops

Rice and maize are the two major summer crops covering almost 50% of the cropland study area. According to crop maps produced using MLC at the end of the season (T8), when maximum accuracy is achieved, 297.7 km^2 and 1240.3 km^2 are classified as Rice and Maize, respectively; the CUAA 2013 map provides similar figures with 297.9 km^2 and 1435.4 km^2, respectively.

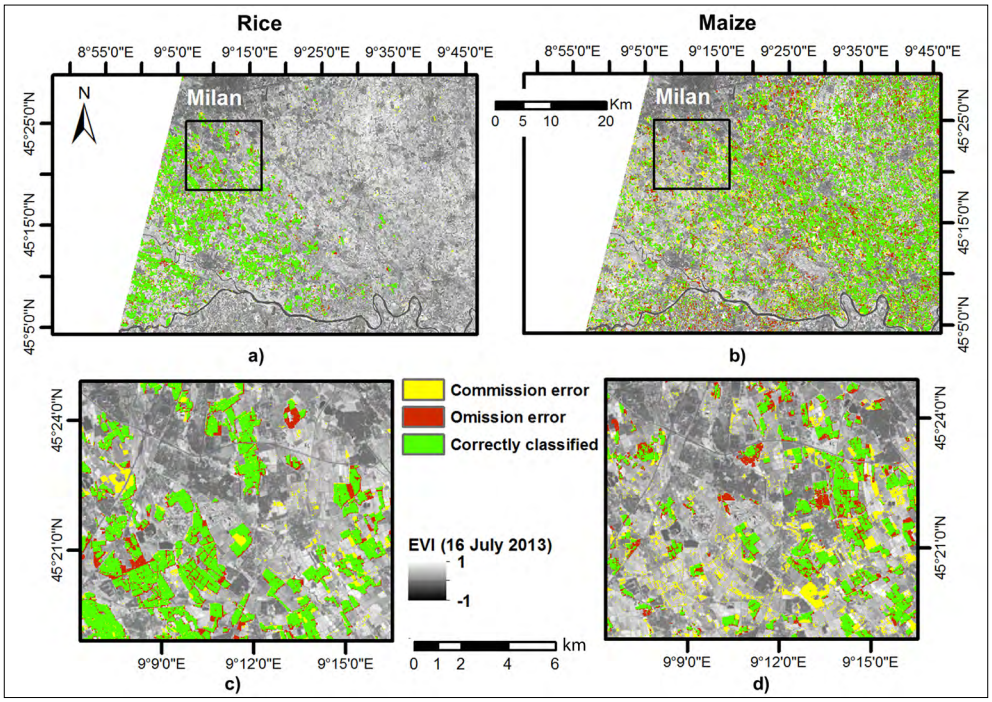

Figure 6 - Spatial patterns of the class errors (red=omission, yellow=commission) and agreement (green) with reference data (CUAA2013), derived from MLC crop maps produced at time step T8 for (a) Rice (OE=0.3%; CE=2.2%) and (b) Maize (OE=4.4%; CE=8.4%) classes. Background is represented by EVI of July 16th, 2013. A detailed view of errors and agreement patterns for the area located southeast of Milan city is provided in (c) for Rice, and (d) for Maize classes.

Figure 6 shows the CE and OE distribution of the Rice and Maize classes as derived from the MLC classification at time step T8 over the study area (Fig. 6a-b) and a detail view over the agricultural region south of Milan city (Fig. 6c-d); errors are derived by comparison to the CUAA 2013 map product. The agreement patches (green colour) correctly identify the known patterns of the areas cultivated with rice and maize. For what concerns the Rice class, no evident pattern of omission and commission errors is present at regional scale (Fig. 6a), while for Maize a significant proportion of the OE (red areas) is located in the agricultural regions East and South-east of Milan city, where the agricultural landscape is very fragmented with small fields. CE (yellow areas) are instead concentrated South of Milan city, where soybean and double crop fields are erroneously classified as Maize.

In general, Rice is the most accurately identified crop class across algorithms and time steps, with CE lower than 10% for all time steps and MLC, NN and SAM classification algorithms (Fig. 5) and OE below 10% for the MLC and NN. In particular, in the case of MCL classification, CE (OE) is lower than 3.7% (1.2%), after T3.
For Maize, CE is generally greater than OE for all time steps and algorithms. MLC shows the lowest difference between CE and OE; the commission error at T1 is above 40% for SAM. The confusion matrices at T2 and T8 (Tab. 4) show that the Maize class is often confused with Soybean and Double crop (i.e. winter crop followed by summer crop, which could also be maize).

Discussion

Results described in previous section showed that among the four supervised algorithms tested for in-season crop type mapping using optical satellite data, MLC is the best performing over the various time steps, with OA above 86.5% already in the middle of July (T2), and reaching OA=92.7% when using the whole multi-temporal dataset (T8). This confirms previous studies, which showed that MLC can achieve good performance for mapping crop types with medium resolution satellite data [Yang et al., 2011; Foerster et al., 2012]. Distance-based classifiers (EMD and SAM) confirmed their underperformance compared to statistical and non-parametric algorithms (MLC and NN). This is probably due to EMD and SAM lacking capabilities in handling intra-class variance into the classification decision rules [South et al., 2004], and in their original design being based on spectral rather than multi-temporal information [Kruse et al., 1993; South et al., 2004]. Moreover, SAM invariance to relative magnitude of input features is possibly adding some confusion when inputs are multi-temporal VIs profiles [Kruse et al., 1993].
MCL requires the availability of training data, which could limit its operational implementation; alternative approaches could be rule-based classifiers exploiting spectral-temporal profiles and synthetic features as input. These methods do not require re-training at each run thus making the methodological approach more suitable for operational implementation over large areas and longer periods [e.g. Foerster et al., 2012]. The use of these approaches and the integration of SAR data, not affected by cloud cover that often limits optical data usability during spring-early summer season in temperate regions, could further enhance early/mid-season crop mapping applications [e.g. Villa et al., 2015].
Although accuracies are generally increasing along the summer season with the addition of each time step, meaning that adding a satellite image at each step brings new information

for mapping target crop types, minor absolute changes are observed (lower than 1.5%) after T3, when all algorithms reach a plateau. As expected, the greatest accuracy increase occurs at the beginning of the season, when the number of images in the multi-temporal stack is lower and summer crop biomass growth is faster; the largest increment is observed between T1 and T2 (middle of July) for all classifiers. This suggests that the OLI scene acquired until the middle of July contains key information related to crop types, which provides a notable enhancement in separating target classes, especially for summer crops. Major summer crops in Lombardy (e.g. rice, maize and soybean) usually reach a peak in vigour during July, following a first stage of fast biomass growth, which starts in late May to the middle of June. These phenological features are well reflected into the evolution of the VIs chosen, thus bringing to a relevant enhancement of accuracy (using MLC) in T2, reaching OA=86.5% ($\boldsymbol{k}$=0.84), compared to OA=78.0% ($\boldsymbol{k}$=0.74) scored at T1. A further gain in crop phenology information, reflected into the increment in crop mapping accuracy using MLC, is observed adding end of July OLI scene (T3), i.e. reaching OA=88.5%, 2% higher than at T2, even if less relevant than for T2-T1 accuracy increment.

A crop map for the study area, which distinguishes seven crop types, can be therefore delivered early (middle of July) during the summer crop growing season using multi-temporal acquisition of mid resolution optical satellite data, i.e. three and a half months after the summer crop season start, with high accuracy levels [Foody, 2002] (OA>85%, $\boldsymbol{k}$>0.82). This early in-season crop map, produced five months ahead of the end of season, could be useful to support agricultural practices and management for the maximization of crop productivity, i.e. for public agencies in charge of water supply and regulation. This result strengthens the findings of previous studies by confirming that: i) the optimal time range for distinguishing summer crops with Landsat occurs from 140 days after the nominal start of growing season [Van Niel and McVicar, 2004], and ii) OA higher than 85% can be achieved for a crop map produced using satellite optical time series around four months after the major summer crop sowing period [Conrad et al., 2014].

Per-class errors tend to group into three distinct patterns: Maize and Forages show a slight overestimation error (CE>OE), Double crop, Soybean and Arboriculture-woodland show inverse trends towards underestimation (OE<CE), and Rice and Winter crop show balanced commission and omission errors. Consistently with what observed for global metrics, OA and $\boldsymbol{k}$, the greatest errors are observed at T1, followed by the most significant reduction rate occurring from T1 to T2.

Rice is among all the best identified class, with CE and OE in the MCL classification lower than 2% after T3. This is due to specific rice crop features: i) in Northern Italy, the rice-cultivated area is clustered in homogeneous regions and fields have an average size greater than 1.5 ha [Giuca et al., 2014], compared to other, more fragmented, agricultural districts within the study area, and ii) the distinct temporal signature of agronomic flooding [Xiao et al., 2005; Boschetti et al., 2014] and the single crop cycle typical of rice cultivations in temperate areas are relatively easy to track with multi-temporal spectral data.

Maize, although being characterized by acceptable errors, is misclassified as Soybean at the beginning of the season, up to T3. Too few information is available to distinguish these classes, which are sown in the same period and are characterised by similar growing rates in the early stages, before late July - beginning of August (T3-T4); hence more images are needed to highlight the difference between the two classes. Furthermore, since maize

cultivation is widespread and presents a great variability in terms of agronomic practices and sowing dates (i.e. maize grown for grain, for silage stocks, or for biogas production), it is possible that some of this heterogeneity is underrepresented in the training set, which can justify the greater errors compared to the other major summer crop types.
Patterns of classification error for Maize (Fig. 6d), include few patches recognised as entire fields and the majority of the misclassification is due to border effects and mixture occurring at the edge of the fields. This aspect suggest that object-based approaches could provide an improvement, especially if a reliable database of field parcels is available [e.g. Ortiz et al., 1997; De Wit and Clevers, 2004].
Other classes are sensitive to the length of the multi-temporal dataset. Double crop class is underestimated (see Fig. 4b, Tab. 4) at the beginning of the season (T1-T2), because it is early to observe the second cycle, which is typically sown around June. However, it is important to remind that crop types (winter crop, soybean), confused with Double crop in satellite maps, are one of the seasonal components of this cropping system in the study area.
Forages class shows an anomalous behaviour, which features an increment in class error from T4 with EMD and SAM, likely due to agronomic practises such as meadows mowing and harvesting, which occur from July to August.
Major crops (rice and maize) acreage estimation (Fig. 6) performed using crop maps produced with MLC at the end of the season are precise enough, especially considering that reference data (CUAA 2013) comprises fields cropped with maize as second crop, which satellite produced crop maps identify as a separated class (Double crop).
The experimental design, focusing on the overlap area between the two adjacent WRS-2 paths, enabled us to exploit the maximum temporal resolution currently provided by medium resolution operational satellites, so that our results could represent a hint about the potential of the forthcoming space platforms hosting similar multi-spectral sensors, i.e. Sentinel-2. Moreover, even if our findings are relative to Lombardy region crop types and practices, our approach could be tested and easily adapted using similar temporal resolution dataset over agricultural areas with climatic and agronomic characteristics similar to Northern Italy. Lombardy climate, characterized by cold winters and hot summers, allows the cultivation of both rain fed winter crops (wheat and barley), and irrigated summer crops (rice and maize). The presence in the study area of different cropping systems and up to seven main crop types indicate that the obtained results could be generalised to other similar context, e.g. temperate and continental Europe.
New generation satellite platforms, such as the Sentinel-2 constellation fully operational by 2017 (with Sentinel-2A now in orbit and regularly acquiring data from the summer of 2015) will soon provide a temporal resolution (10 days with one sensor and 5 days with full two-satellite constellation) that will further enhance crop mapping based on multi-temporal approaches. Indeed, the synergic use of OLI data with future Sentinel-2A data, which spectral configuration allow to derive the VIs used in our approach should ensure a high temporal revisit with of less than 10 days, enhancing the potential frequency of cloud free scenes. When both Sentinel-2 satellites will be operational (expected in 2017), with the increment in time revisit (less than 5 days, adding Landsat 8 data) and the spectral bands in the red-edge range, a boost in crop mapping reliability the production of even earlier crop maps (possibly in late June) will become feasible, thus further increasing the potential for operational crop management.

Conclusions

In this work, we analysed the performance of crop classification from multi-temporal Landsat 8 OLI images over a study area in Northern Italy. Four supervised classification algorithms applied to spectral indices (EVI, NDFI, RGRI) profiles have been tested over different time step datasets, to assess the performance of in-season crop classification in the year 2013. Maximum Likelihood gave most accurate classification results and a crop type map with seven classes with OA=86.5% was produced five months ahead of the end of season, in the middle of July.

Our findings demonstrate that near real-time, in season crop mapping is feasible using satellite data with suitable spatial and temporal resolution in a simple, operational and inexpensive way. This early in-season crop map could be useful to support agricultural practices and management, especially for supporting the analysis of water demand for major crops (rice and maize) during dry summer months.

Acknowledgements

This work has been conducted in the frame of Space4Agri research project funded and supported by the AQ CNR-Regione Lombardia (CNR, Convenzione Operativa n. 18091/RCC, 05/08/2013).

References

Boschetti M., Nutini F., Manfron G., Brivio P.A., Nelson A. (2014) - *Comparative Analysis of Normalised Difference Spectral Indices Derived from MODIS for Detecting Surface Water in Flooded Rice Cropping Systems*. PloS one, 9 (2): e88741. doi: http://dx.doi.org/10.1371/journal.pone.0088741.

Congalton R.G. (1991) - *A review of assessing the accuracy of classifications of remotely sensed data*. Remote Sensing of Environment, 37 (1): 35-46. doi: http://dx.doi.org/10.1016/0034-4257(91)90048-B.

Conrad C., Dech S., Dubovyk O., Fritsch S., Klein D., Löw F. Zeidler J. (2014) - *Derivation of temporal windows for accurate crop discrimination in heterogeneous croplands of Uzbekistan using multitemporal RapidEye images*. Computers and Electronics in Agriculture, 103: 63-74. doi: http://dx.doi.org/10.1016/j.compag.2014.02.003.

De Wit A.J.W., Clevers J.G.P.W. (2004) - *Efficiency and accuracy of per-field classification for operational crop mapping*. International Journal of Remote Sensing, 25 (20): 4091-4112. doi: http://dx.doi.org/10.1080/01431160310001619580.

Drusch M., Del Bello U., Carlier S., Colin O., Fernandez V., Gascon F., Hoersch B., Isola C., Laberinti P., Martimort P., Meygret A., Spoto F., Sy O., Marchese F., Bargellini P. (2012) - *Sentinel-2: ESA's Optical High-Resolution Mission for GMES Operational Services*. Remote Sensing of Environment, 120: 25-36. doi: http://dx.doi.org/10.1016/j.rse.2011.11.026.

Duveiller G., Defourny P. (2010) - *A conceptual framework to define the spatial resolution requirements for agricultural monitoring using remote sensing*. Remote Sensing of Environment, 114 (11): 2637-2650. doi: http://dx.doi.org/10.1016/j.rse.2010.06.001.

Foerster S., Kaden K., Foerster M., Itzerott S. (2012) - *Crop type mapping using spectral-*

temporal profiles and phenological information. Computers and Electronics in Agriculture, 89: 30-40. doi: http://dx.doi.org/10.1016/j.compag.2012.07.015.

Foody G.M. (2002) - *Status of land cover classification accuracy assessment*. Remote Sensing of Environment, 80 (1): 185-201. doi: http://dx.doi.org/10.1016/S0034-4257(01)00295-4.

Gamon J.A., Penuelas J., Field C.B. (1992) - *A narrow-waveband spectral index that tracks diurnal changes in photosynthetic efficiency*. Remote Sensing of Environment, 41 (1): 35-44. doi: http://dx.doi.org/10.1016/0034-4257(92)90059-S.

Gamon J.A., Surfus J.S. (1999) - *Assessing Leaf Pigment Content and Activity with a Reflectometer*. New Phytologist, 143: 105-117. doi: http://dx.doi.org/10.1046/j.1469-8137.1999.00424.x.

Giuca S., Giannini M.S., Nebuloni A., Pretolani R., Pieri R., Cagliero R., Marras F., Gay G. (2014) - *Lombardy agriculture in figures - 2013*. National Institute of Agricultural Economics (INEA), 156 pp. Available online at: http://dspace.inea.it/bitstream/inea/846/1/Lombardy_agric_figures_2013.pdf.

Gitelson A.A., Merzlyak M.N. (1996) - *Signature analysis of leaf reflectance spectra: algorithm development for remote sensing of chlorophyll*. Journal of Plant Physiology, 148 (3): 494-500. doi: http://dx.doi.org/10.1016/S0176-1617(96)80284-7.

Hartfield K.A., Marsh S.E., Kirk C.D., Carrière Y. (2013) - *Contemporary and historical classification of crop types in Arizona.* International Journal of Remote Sensing, 34 (17): 6024-6036. doi: http://dx.doi.org/10.1080/01431161.2013.793861.

Huete A., Justice C., Liu H. (1994) - *Development of vegetation and soil indices for MODIS-EOS*. Remote Sensing of Environment, 49 (3): 224-234. doi: http://dx.doi.org/10.1016/0034-4257(94)90018-3.

Huete A.R., Liu H., Batchily K., van Leeuwen W. (1997) - *A comparison of vegetation indices over a global set of TM images for EOS-MODIS*. Remote Sensing of Environment, 59: 440-451. doi: http://dx.doi.org/10.1016/S0034-4257(96)00112-5.

Hubert-Moy L., Cotonnec A., Le Du L., Chardin A., Perez P. (2001) - *A comparison of parametric classification procedures of remotely sensed data applied on different landscape units.* Remote Sensing of Environment, 75: 174-187. doi: http://dx.doi.org/10.1016/S0034-4257(00)00165-6.

Kruse F.A., Lefkoff A.B., Boardman J.B., Heidebrecht K.B., Shapiro A.T., Barloon P.J., Goetz A.F.H. (1993) - *The spectral image processing system (SIPS)-interactive visualization and analysis of imaging spectrometer data.* Remote Sensing of Environment, 44 (2): 145-163. doi: http://dx.doi.org/10.1016/0034-4257(93)90013-N.

Irons J.R., Dwyer J.L., Barsi J.A. (2012) - *The next Landsat satellite: The Landsat Data Continuity Mission*. Remote Sensing of Environment, 122: 11-21. doi: http://dx.doi.org/10.1016/j.rse.2011.08.026.

Lunetta R.S., Knight J.F., Ediriwickrema J., Lyon J.G., Worthy L.D. (2006) - *Land-cover change detection using multi-temporal MODIS NDVI data*. Remote Sensing of Environment, 105 (2): 142-154. doi: http://dx.doi.org/10.1016/j.rse.2006.06.018.

Mo X., Liu S., Lin Z., Xu Y., Xiang Y., McVicar T.R. (2005) - *Prediction of crop yield, water consumption and water use efficiency with a SVAT-crop growth model using remotely sensed data on the North China Plain*. Ecological Modelling, 183 (2): 301-322. doi: http://dx.doi.org/10.1016/j.ecolmodel.2004.07.032.

Murthy C.S., Raju P.V., Badrinath K.V.S. (2003) - *Classification of wheat crop with multi-temporal images: performance of maximum likelihood and artificial neural networks,* International Journal of Remote Sensing, 24 (23): 4871-4890. doi: http://dx.doi.org/10.1080/0143116031000070490.

Nutini F., Boschetti M., Brivio P.A., Bocchi S., Antoninetti M. (2013) - *Land-use and land-cover change detection in a semi-arid area of Niger using multi-temporal analysis of Landsat images*. International Journal of Remote Sensing, 34 (13): 4769-4790. doi: http://dx.doi.org/10.1080/01431161.2013.781702.

Odenweller J.B., Johnson K.I. (1984) - *Crop identification using Landsat temporal-spectral profiles.* Remote Sensing of Environment, 14 (1): 39-54. doi: http://dx.doi.org/10.1016/0034-4257(84)90006-3.

Ok A.O., Akar O., Gungor O. (2012) - *Evaluation of random forest method for agricultural crop classification.* European Journal of Remote Sensing, 45 (3): 421-432. doi: http://dx.doi.org/10.5721/EuJRS20124535.

Ortiz M.J., Formaggio A.R., Epiphanio J.C.N. (1997) - *Classification of croplands through integration of remote sensing, GIS, and historical database*. International Journal of Remote Sensing, 18 (1): 95-105. doi: http://dx.doi.org/10.1080/014311697219295.

Pohl C., Van Genderen J.L. (1998) - *Multisensor image fusion in remote sensing: concepts, methods and applications*. International Journal of Remote Sensing, 19 (5): 823-854. doi: http://dx.doi.org/10.1080/014311698215748.

Reichstein M., Ciais P., Papale D., Valentini R., Running S., Viovy N., Cramer W., Granier A., Ogée J., Allard V., Aubinet M., Bernhofer C., Buchmann N., Carrara A., Grunwald T., Heimann M., Heinesch B., Knohl A., Kutsch W., Loustau D., Manca G., Matteucci G., Miglietta F., Ourcival J.M., Pilegaard K., Pumpanen J., Rambal S., Schaphoff S., Seufert G., Soussana J.-F., Sanz M.-J., Vesala T., Zhao M. (2007) - *Reduction of ecosystem productivity and respiration during the European summer 2003 climate anomaly: a joint flux tower, remote sensing and modelling analysis.* Global Change Biology, 13 (3): 634-651. doi: http://dx.doi.org/10.1111/j.1365-2486.2006.01224.x.

Richards J.A. (1999) - *Remote Sensing Digital Image Analysis*. Springer-Verlag, Berlin, p. 240.

Richter R., Schläpfer D. (2011) - *Atmospheric / Topographic Correction for Satellite Imagery*. DLR report DLR-IB 565-02/11, Wessling (D), pp 202. Available online at: http://atcor.com/pdf/atcor3_manual.pdf.

Rost S., Gerten D., Bondeau A., Lucht W., Rohwer J., Schaphoff S. (2008) - *Agricultural green and blue water consumption and its influence on the global water system.* Water Resources Research, 44 (9): W09405. doi: http://dx.doi.org/10.1029/2007WR006331.

South S., Qi J., Lusch D.P. (2004) - *Optimal classification methods for mapping agricultural tillage practices*. Remote Sensing of Environment, 91 (1): 90-97. doi: http://dx.doi.org/10.1016/j.rse.2004.03.001.

Van Niel T.G., McVicar T.R. (2004) - *Determining temporal windows for crop discrimination with remote sensing: a case study in south-eastern Australia.* Computers and Electronics in Agriculture, 45 (1): 91-108. doi: http://dx.doi.org/10.1016/j.compag.2004.06.003.

Villa P., Bresciani M., Braga F., Bolpagni R. (2014) - *Comparative assessment of broadband Vegetation Indices over aquatic vegetation.* IEEE Journal of Selected Topics in Applied Earth Observations and Remote Sensing, 7 (7): 3117-3127. doi: http://dx.doi.

org/10.1109/JSTARS.2014.2315718.

Villa P., Stroppiana D., Fontanelli G., Azar R., Brivio P.A. (2015) - *In-season mapping of crop type with optical and X-band SAR data: a classification tree approach using synoptic seasonal features*. Remote Sensing, 7 (10): 12859-12886. doi: http://dx.doi.org/10.3390/rs71012859.

Wardlow B.D., Egbert S.L. (2008) - *Large-area crop mapping using time-series MODIS 250 m NDVI data: An assessment for the US Central Great Plains.* Remote Sensing of Environment, 112 (3): 1096-1116. doi: http://dx.doi.org/10.1016/j.rse.2007.07.019.

Wriedt G., Van der Velde M., Aloe A., Bouraoui F. (2009) - *Estimating irrigation water requirements in Europe.* Journal of Hydrology, 373 (3): 527-544. doi: http://dx.doi.org/10.1016/j.jhydrol.2009.05.018.

Xiao X., Boles S., Liu J., Zhuang D., Frolking S., Li C., Salas L., Moore B. (2005) - *Mapping paddy rice agriculture in southern China using multi-temporal MODIS images*. Remote Sensing of Environment, 95 (4): 480-492. doi: http://dx.doi.org/10.1016/j.jhydrol.2009.05.018.

Yang C., Everitt J.H., Murden D. (2011) - *Evaluating high resolution SPOT 5 satellite imagery for crop identification.* Computers and Electronics in Agriculture, 75 (2): 347-354. doi: http://dx.doi.org/10.1016/j.compag.2010.12.012.